

Anomalous Suppression of Valley Splittings in Lead Salt Nanocrystals without Inversion Center

A.N. Poddubny,¹ M.O. Nestoklon,¹ S.V. Goupalov^{1,2}

¹*Ioffe Physical-Technical Institute, 26 Polytekhnicheskaya St., 194021 St. Petersburg, Russia*

²*Department of Physics, Jackson State University, Jackson, Mississippi 39217, USA*

Atomistic $sp^3d^5s^*$ tight-binding theory of PbSe and PbS nanocrystals is developed. It is demonstrated, that the valley splittings of confined electrons and holes strongly and peculiarly depend on the geometry of a nanocrystal. When the nanocrystal lacks a microscopic center of inversion and has T_d symmetry, the splitting is strongly suppressed as compared to the more symmetric nanocrystals with O_h symmetry, having an inversion center.

PACS numbers: 71.35.-y, 71.36.+c, 42.70.Qs

Interest in almost spherical nanocrystals (NCs) made of lead chalcogenides (PbSe, PbS) has recently exploded due to their utility in fundamental studies of quantum confinement effects and enabling potential for technological applications in photovoltaics [1–4]. These applications impose requirements of reproducibility of the devices, ability to control their properties and necessity to understand mechanisms behind physical processes underlying their work. It has been noted [5, 6] that lead salt NCs are very peculiar compared to quantum dots (QDs) of III-V and II-VI compound semiconductors because lead chalcogenides have band extrema in the four inequivalent L -points of the Brillouin zone and such effects as confinement-induced valley-mixing and effective mass anisotropy should be considered to fully account for the properties of lead salt NCs. It also was suggested that optical properties of lead salt NC QDs can be sensitive to a particular arrangement of atoms within the QD, as the latter determines the overall symmetry of the structure [7, 8].

In this work we study how all these effects influence the valley-orbit and spin-orbit splittings of one-particle energy levels of electrons and holes confined in lead salt NCs using the atomistic tight-binding (TB) approach. We found that these splittings are very sensitive to the particular arrangement of atoms within the almost spherical NC. In particular, we considered NCs of almost spherical shape centered on an anion or cation atom, serving as a center of inversion, along with NCs having no inversion symmetry. We found that in NCs without a center of inversion the valley-orbit and spin-orbit splittings of electron energy levels are strongly suppressed. This effect is quite unusual because typically a higher symmetry of a physical system implies a higher degeneracy of its energy levels, while in our case the suppression of the splittings occurs in NCs having lower symmetry. Nevertheless, we were able to explain this puzzling behavior using mathematical apparatus of the group theory.

Lead chalcogenides (PbSe, PbS) are semiconductor compounds with a rocksalt crystal lattice and a narrow and direct band gap [9]. The extrema of both the conduc-

tion and valence bands are located at the four L -points of the Brillouin zone:

$$\mathbf{k}_{1,2} = \frac{\pi}{a} (1, \pm 1, \pm 1), \quad \mathbf{k}_{3,4} = \frac{\pi}{a} (-1, \pm 1, \mp 1), \quad (1)$$

where a is the lattice constant. The empirical TB method is an efficient tool to model electronic properties of large-scale nanostructures [10]. Success of the TB parametrization depends on the choice of basis functions and on the accuracy of the fit of the bulk band structure. The simplest TB parametrizations of lead chalcogenides are based on the basis set of the three p orbitals playing major role in the formation of the valence and conduction band states [11, 12]. More quantitatively accurate models include also s^* and d orbitals [5, 13–15]. However, no attempts (with the only exception of Ref. [12]) have been made to fit the actual effective masses of the electrons and holes near the L -points. On the other hand, the second-nearest neighbors p^3 model of Ref. [12] fails to reproduce the bulk dispersion for wavevectors far from the L points [6]. Consequently, even the most advanced existing TB parametrizations of lead chalcogenides [5] are not suitable [16] for an adequate description of the NCs.

We have performed an independent atomistic $sp^3d^5s^*$ TB parametrization of the electron energy dispersion in bulk PbSe and PbS by fitting the spectra calculated by the state-of-the-art GW technique of Ref. [17]. The goal values for the carrier effective masses near the L -points were set to the experimental values [18]: $m_{c,l}^{exp} = 0.070 m_0$, $m_{c,t}^{exp} = 0.040 m_0$, $m_{h,l}^{exp} = 0.068 m_0$, $m_{h,t}^{exp} = 0.034 m_0$ for PbSe and $m_{c,l}^{exp} = 0.105 m_0$, $m_{c,t}^{exp} = 0.080 m_0$, $m_{h,l}^{exp} = 0.105 m_0$, $m_{h,t}^{exp} = 0.075 m_0$ for PbS (m_0 is the free electron mass), as even the modern *ab initio* approach [17] does not satisfactorily reproduce the effective masses.

The TB parameters we obtained are listed in Table I. The resulting effective masses $m_{c,l} = 0.068 m_0$, $m_{c,t} = 0.041 m_0$, $m_{h,l} = 0.069 m_0$, $m_{h,t} = 0.039 m_0$ for PbSe and $m_{c,l} = 0.098 m_0$, $m_{c,t} = 0.079 m_0$, $m_{h,l} = 0.104 m_0$, $m_{h,t} = 0.074 m_0$ for PbS are quite close to the experimental values. The spin-orbit coupling constants of p orbitals at Pb, Se, and S were not changed during the

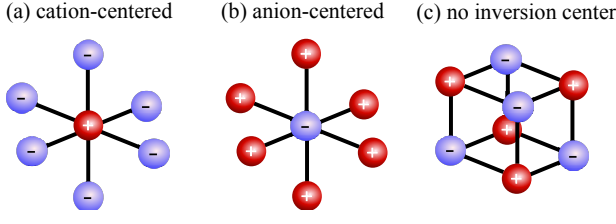


FIG. 1: Central parts of the three types of nanocrystals.

fitting procedure and were taken from Refs. [21] and [22] for Pb and for the anions, respectively.

In our study we will consider the three types of NC geometries illustrated in Fig. 1. For the structures shown in Figs. 1a(b) the center of the spherical NC is on a cation (anion) atom while for the structure in Fig. 1c the center of the sphere lies halfway between a cation and an anion on a line parallel to the [111] direction. The non-stoichiometric QDs of the types (a) and (b) both have centers of inversion and are characterized by the cube symmetry group O_h . The stoichiometric QD of the type (c) has no inversion center and is characterized by the tetrahedron symmetry group T_d . Note that the QDs cannot be perfectly spherical due to the discreteness and lower point symmetry of the underlying crystal lattice. In our work the QDs are formed by all the atoms within a certain distance from the center of the NC. It is convenient to measure this distance with a dimensionless integer number. Thus, we define the “number of shells” as

TABLE I: TB parameters for PbSe and PbS. The transfer integrals are measured in eV and given in the Slater-Koster notations [19]. The spin-orbit splittings are defined according to Ref. [20].

	PbS	PbSe		PbS	PbSe
$a_0, \text{\AA}$	5.900	6.100	$s_a^* p_c \sigma$	2.606	2.258
E_{sa}	-10.596	-10.722	$s_c^* p_a \sigma$	2.177	1.731
E_{sc}	-5.444	-6.196	$s_a d_c \sigma$	-1.852	-1.917
E_{pa}	-1.797	-1.463	$s_c d_a \sigma$	-1.399	-1.256
E_{pc}	4.819	4.279	$s_a^* d_c \sigma$	0.040	0.146
E_{da}	7.468	7.984	$s_c^* d_a \sigma$	-0.792	-0.271
E_{dc}	20.900	26.114	$pp\sigma$	2.223	2.159
E_{s^*a}	17.878	15.117	$pp\pi$	-0.468	-0.463
E_{s^*c}	25.807	28.244	$p_a d_c \sigma$	-1.200	-1.272
$ss\sigma$	-0.567	-0.292	$p_c d_a \sigma$	-1.219	-1.332
$s^* s^* \sigma$	-2.478	-1.346	$p_a d_c \pi$	0.442	0.912
$s_c s_a^* \sigma$	-1.535	-0.654	$p_c d_a \pi$	0.983	0.966
$s_a s_c^* \sigma$	-0.693	-1.743	$dd\sigma$	0.778	0.244
$s_a p_c \sigma$	1.623	1.611	$dd\pi$	1.202	1.826
$s_c p_a \sigma$	1.371	1.291	$dd\delta$	-1.305	-1.235
Δ_a	0.096	0.420	Δ_c	2.380	2.380

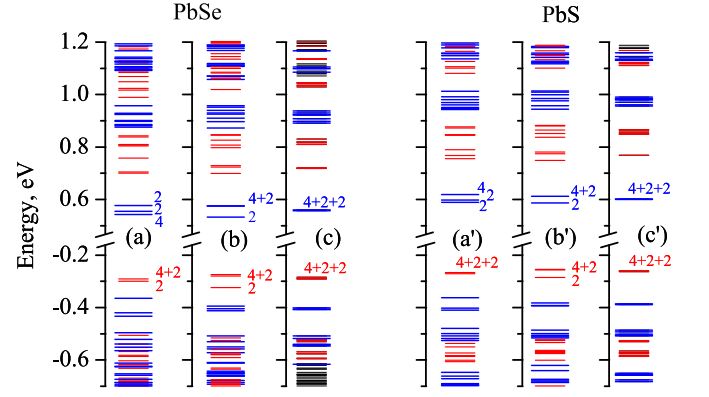


FIG. 2: (Color online) Energy levels in PbSe (a,b,c) and PbS (a',b',c') NCs with diameter $D \approx 4.9$ nm and $D \approx 4.6$ nm, respectively. Panels (a–c) and (a'–c') correspond to cation-centered NCs, anion-centered NCs and NCs without an inversion center, respectively (see Fig. 1). States of the odd and even parity are marked by the long thick blue and short thick red lines, respectively. The thin black lines correspond to the states without a certain parity. The degeneracies of the lowest electron and hole confined states are indicated near each line.

the number of atomic layers within the distance from the center of the QD to its surface along the [100] direction.

Contrary to covalent semiconductors like Si [5], lead chalcogenides are characterized by the strongly ionic atomic bonds making them relatively insensitive to the surface chemistry [16]. In particular, no surface states appear in the fundamental band gap of non-passivated lead chalcogenide NCs. Therefore, we have not passivated the surface atoms in our TB modeling. In real QDs of the types (a) and (b) (cf. Fig. 1) such passivation is necessary to compensate for the surface charge [23]. The actual structure of the NCs should depend on the details of the synthesis procedure and can be determined with the help of the nuclear magnetic resonance[24] and X-ray diffraction[25] techniques.

The calculated energy levels of confined carriers for PbSe and PbS NCs of the diameter $D \approx 5$ nm (corresponding to 9 shells) are shown in Fig. 2. For each material three panels (a–c and a'–c') correspond to the three possible NC geometries illustrated in Fig. 1. The band gap in both cases agrees well with the results of Ref. [5].

All the states can be divided into distinct groups characterized by a certain parity. For NCs with a center of inversion, each state automatically has a certain parity. Indeed, in bulk lead chalcogenides the lowest electron state in the conduction band has the L_6^- symmetry [17], *i.e.* it is odd with respect to the inversion symmetry operation when the center of inversion is chosen on the cation atom. The uppermost electron state in the valence band has the opposite parity. For QDs without an

inversion center one can define approximate projectors to the even and odd states. We have attributed a certain parity to the states, for which the squared mean values of the projectors differed more than in three times.

Energy splittings within each multiplet characterized by a certain parity are clearly seen in Fig. 2 and can be explained by the confinement-induced inter-valley coupling and the carrier effective mass anisotropy. The importance of these two effects for lead chalcogenide NCs has been emphasized in Ref. [6]. However, the dependence of the splittings on the NC geometry clearly manifested in Fig. 2 has never been reported.

A striking feature of Fig. 2 is the suppression of the energy splittings for the type (c) NCs lacking a center of inversion. The splittings are quite small and cannot be distinguished within the energy scale of Fig 2. On the contrary, for QDs with an inversion center [panels (a), (b), (a'), (b') of Fig. 2], the ground-state multiplets for both electrons and holes have well-pronounced structures with substantial splittings even for QD diameters as large as 4.9 nm. This observation refers to both the conduction and valence band electron states. The effect is more pronounced for the PbS QDs than for the PbSe QDs, which can be related to the more isotropic effective masses of the band extrema in bulk PbS.

To elucidate this puzzling behavior, we have analyzed the dependence of the splittings on the NC diameter. For simplicity, we restrict our consideration by the electron and hole ground states. Within the effective mass approximation, the ground state of confined carriers is fourfold degenerate with respect to the valley index and twofold degenerate with respect to the spin projection, *i.e.* the total degeneracy is eightfold. If we neglect the spin and consider valley-orbit interaction only, the ground state is split into a state of A_1 symmetry (singlet), and a state of F_2 symmetry (triplet), as sketched in insets of Figs. 3,4. When the spin degree of freedom is taken into account then both the singlet and the triplet states acquire extra degeneracy. This degeneracy is partly lifted, as the six-fold degenerate state corresponding to the triplet is split by the spin-orbit interaction into a two-fold degenerate state of E'_2 symmetry and a four-fold degenerate state of G' symmetry [26]. As a result, the carrier ground-state level is split into the three multiplets: the two doublets (of E'_1 and E'_2 symmetry, respectively) and the four-fold degenerate state of G' symmetry. As far as the symmetry with respect to inversion is not concerned, the symmetry groups T_d and O_h are equivalent. Therefore, this symmetry analysis applies to all types of NC geometries presented in Fig. 1.

Figures 3 and 4 show the energies of the resulting conduction (valence) band multiplets in PbS NCs as functions of the NC diameter. The panels (a)–(c) correspond to the three NC geometries considered throughout the paper (see Fig. 1). The energies of the states are counted

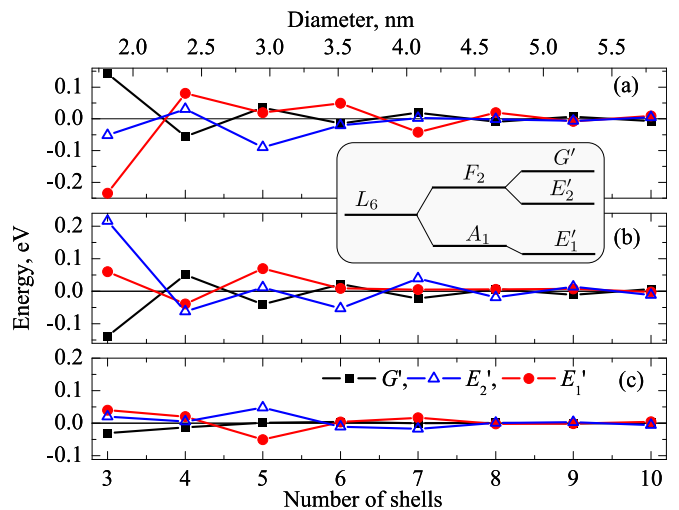


FIG. 3: (Color online) Energies of levels belonging to the ground state multiplet of the conduction band electron in PbS NCs as functions of NC diameter. Panels (a), (b), (c) correspond to Pb-centered NCs, S-centered NCs and NCs without inversion center, see Fig. 1. Squares, triangles and circles correspond to the states with the symmetry G' , E'_2 and E'_1 , respectively, see the level splitting scheme in the inset.

from the averaged value $(E_{E'_1} + E_{E'_2} + 2E_{G'})/4$. The splittings strongly oscillate with the number of shells N in a NC. Such oscillations are typical for the valley splittings in various semiconductor structures. Similar behavior has been reported for SiGe/Si[27, 28] and GaSb/AlAs[29, 30] quantum wells and Si NCs [31].

Comparison of panels (a) and (b) of Figs. 3,4 on one hand with the panels (c) of Figs. 3,4 on the other hand clearly shows that the suppression of valley splittings in NCs without a center of inversion is a general feature persistent in a wide range of NC sizes. Comparison of Fig. 3

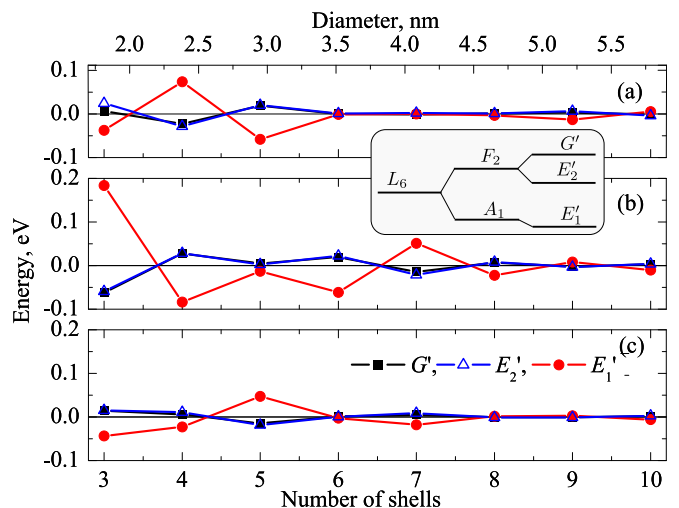


FIG. 4: (Color online) Same as Fig. 3, but for the valence band ground state.

with Fig. 4 enables one to conclude that the spin-orbit interaction is much stronger for conduction-band electrons than for valence-band holes. Indeed, the energies of the hole states with the symmetry G' and E'_2 in Fig. 4 are almost the same, while, for conduction-band electrons, all the splittings in Fig. 3 are of the same order.

Let us explain the anomalous suppression of the valley splittings in lead salt NCs without an inversion center. We want to account for the inter-valley coupling in the lowest non-vanishing approximation. To this end we consider electronic states originating from the four inequivalent L valleys of a bulk semiconductor and neglect the $\mathbf{k}\cdot\mathbf{p}$ mixing of conduction and valence band states [9]. Then the wave function of the confined electron state in the j -th L -valley can be written as $\langle \mathbf{r} | L_j \rangle = e^{i\mathbf{k}_j \cdot \mathbf{r}} u_j(\mathbf{r}) \Phi_j(\mathbf{r})$, where $\Phi_j(\mathbf{r})$ is the smooth envelope function, $u_j(\mathbf{r})$ is the periodic Bloch amplitude for the bulk state in the j -th valley, and spin indices are omitted. We will further assume that the bulk material has isotropic effective masses of the band extrema in L points. In this approximation the envelopes $\Phi_j(\mathbf{r})$ are invariant under rotations. The confinement-induced inter-valley coupling can be described by the following matrix element:

$$I_{j,k} = \langle L_j | H_{\text{QD}} | L_k \rangle, \quad j, k = 1 \dots 4, \quad j \neq k, \quad (2)$$

where H_{QD} is the microscopic QD Hamiltonian. Then it follows that the integral $I_{j,k}$ vanishes when the QD lacks inversion symmetry, *i.e.* belongs to the type (c). To show this let us rewrite $I_{j,k}$ as

$$I_{j,k} \approx \int_{u.c.} e^{-i\mathbf{k}_j \cdot \mathbf{r}} u_j^*(\mathbf{r}) H_{\text{bulk}} e^{i\mathbf{k}_k \cdot \mathbf{r}} u_k(\mathbf{r}) d\mathbf{r} \times \sum_{\mathbf{R}_n} e^{i(\mathbf{k}_k - \mathbf{k}_j) \cdot \mathbf{R}_n} \Phi_j^*(\mathbf{R}_n) \Phi_k(\mathbf{R}_n), \quad (3)$$

where the integral in the right-hand side is over a unit cell and contains the Hamiltonian of a bulk material while the summation runs over all the cation (or anion) sites *within the QD*. It is this summation that is sensitive to the arrangement of atoms within the QD. For the type (c) geometry the sum is exactly zero. This cancellation takes place independently of the radius of the QD and is fully determined by the symmetry. To see this one can use the following well known fact [26]. If a given function describing some crystalline physical system transforms according to a certain representation of the system's symmetry group, then the sum of this function over the lattice sites belonging to the system may be different from zero if and only if the decomposition of this representation into irreducible ones contains the identity representation.

In our case one can distinguish three linearly independent functions $\exp[i(\mathbf{k}_k - \mathbf{k}_j) \cdot \mathbf{R}_n]$ which may be chosen as shown in the first column of Table II. Table II gives the values of these exponent functions when \mathbf{R}_n sweeps the coordinates of the anion atoms shown in Fig. 1(c).

These atoms may be obtained from one another by the rotations of the type (c) QD. The last column of Table II indicates that the exponent functions transform according to the vector irreducible representation F_2 of the group T_d . This representation is different from the identity representation A_1 . Therefore, for type (c) QDs Eq. (3) is zero. Table III gives the values of the same exponent functions when \mathbf{R}_n sweeps the coordinates of the anion atoms shown in Fig. 1(a). These atoms may be obtained from one another by the rotations of the type (a) QD. The last row of Table III shows that the sum of the exponent functions remains invariant under such rotations. More precisely, the exponent functions transform according to the direct sum of the two irreducible representations $A_1^+ \oplus E^+$ of the group O_h . Thus, for type (a) QDs Eq. (3) is different from zero.

TABLE II: Phase factors in Eq. (3) for the coordinates of the anion atoms in Fig. 1(c).

	$\frac{a}{4}(1, 1, 1)$	$\frac{a}{4}(1, \bar{1}, \bar{1})$	$\frac{a}{4}(\bar{1}, 1, \bar{1})$	$\frac{a}{4}(\bar{1}, \bar{1}, 1)$	
$e^{i(\mathbf{k}_1 - \mathbf{k}_2) \cdot \mathbf{R}_n}$	-1	-1	1	1	$-x$
$e^{i(\mathbf{k}_1 - \mathbf{k}_3) \cdot \mathbf{R}_n}$	-1	1	-1	1	$-y$
$e^{i(\mathbf{k}_1 - \mathbf{k}_4) \cdot \mathbf{R}_n}$	-1	1	1	-1	$-z$

TABLE III: Same as Table II but for anion atoms in Fig. 1(a).

	$(\pm \frac{a}{2}, 0, 0)$	$(0, \pm \frac{a}{2}, 0)$	$(0, 0, \pm \frac{a}{2})$	
$e^{i(\mathbf{k}_1 - \mathbf{k}_2) \cdot \mathbf{R}_n}$	1	-1	-1	
$e^{i(\mathbf{k}_1 - \mathbf{k}_3) \cdot \mathbf{R}_n}$	-1	1	-1	
$e^{i(\mathbf{k}_1 - \mathbf{k}_4) \cdot \mathbf{R}_n}$	-1	-1	1	
$\sum_{j=2}^4 e^{i(\mathbf{k}_1 - \mathbf{k}_j) \cdot \mathbf{R}_n}$	-1	-1	-1	A_1^+

This consideration is no longer valid if the function $\Phi_j(\mathbf{r})$ is anisotropic. This is the case of real lead salts NCs, as in bulk lead chalcogenides the longitudinal mass in the L valley is larger than the transverse one. Consequently, in real NCs lacking inversion center the valley splitting is not exactly zero but determined by the degree of the effective mass anisotropy in L valleys. This explains the fact that in PbS NCs the splitting is smaller than in PbSe ones, cf. panels (c) and (c') of Fig. 2.

In conclusion, we obtained a new set of $sp^3d^5s^*$ TB parameters for the bulk PbSe and PbS semiconductor compounds and calculated the electron and hole energy levels in NCs made of these materials. We demonstrated that the valley-orbit and spin-orbit splittings of the ground electron and hole energy levels are very sensitive to a particular arrangement of atoms in the NC and can be strongly suppressed for a certain geometry, when the NC lacks a center of inversion.

Useful discussions with E.L. Ivchenko and L.E. Golub are gratefully acknowledged. This work was supported by the Russian Foundation for Basic Research, European projects POLAPHEN and Spin-Optronics and the "Dy-

nasty” Foundation-ICFPM. The work of SVG was supported, in part, by the Research Corporation for Science Advancement under Award No. 20081 and, in part, by the National Science Foundation under Grant No. HRD-0833178. The work of MON was partially supported by “Triangle de la Physique”.

-
- [1] R. J. Ellingson, M. C. Beard, J. C. Johnson, P. Yu, O. I. Micic, A. J. Nozik, A. Shabaev, and A. L. Efros, *Nano Letters* **5**, 865 (2005).
- [2] R. D. Schaller and V. I. Klimov, *Phys. Rev. Lett.* **92**, 186601 (2004).
- [3] M. T. Trinh, A. J. Houtepen, J. M. Schins, T. Hanrath, J. Piris, W. Knulst, A. P. L. M. Goossens, and L. D. A. Siebbeles, *Nano Letters* **8**, 1713 (2008).
- [4] M. C. Beard, A. G. Midgett, M. Law, O. E. Semonin, R. J. Ellingson, and A. J. Nozik, *Nano Letters* **9**, 836 (2009).
- [5] G. Allan and C. Delerue, *Phys. Rev. B* **70**, 245321 (2004).
- [6] J. M. An, A. Franceschetti, S. V. Dudy, and A. Zunger, *Nano Lett.* **6**, 2728 (2006).
- [7] S. V. Goupalov, *Phys. Rev. B* **79**, 233305 (2009).
- [8] G. Nootz, L. A. Padilha, P. D. Olszak, S. Webster, D. J. Hagan, E. W. Van Stryland, L. Levina, V. Sukhovatkin, L. Brzozowski, and E. H. Sargent, *Nano Lett.* **10**, 3577 (2010).
- [9] I. Kang and F. W. Wise, *J. Opt. Soc. Am. B* **14**, 1632 (1997).
- [10] C. Delerue and M. Lanoo, *Nanostructures. Theory and Modelling* (Springer Verlag, Berlin, Heidelberg, 2004).
- [11] D. L. Mitchell and R. F. Wallis, *Phys. Rev.* **151**, 581 (1966).
- [12] B. Volkov, O. Pankratov, and A. Sazonov, *Soviet J. Experimental and Theoretical Phys.* **58**, 809 (1983).
- [13] C. S. Lent, M. A. Bowen, J. D. Dow, R. S. Allgaier, O. F. Sankey, and E. S. Ho, *Superlattices and Microstructures* **2**, 491 (1986).
- [14] M. Lach-hab, D. A. Papaconstantopoulos, and M. J. Mehl, *J. Phys. Chem. Solids* **63**, 833 (2002).
- [15] J. A. Valdivia and G. E. Barberis, *J. Phys. Chem. Solids* **56**, 1141 (1995).
- [16] A. Paul and G. Klimeck, *Appl. Phys. Lett* **98**, 212105 (2011).
- [17] A. Svane, N. E. Christensen, M. Cardona, A. N. Chantis, M. van Schilfgaarde, and T. Kotani, *Phys. Rev. B* **81**, 245120 (2010).
- [18] H. Preier, *Appl. Phys. A: Materials Sci. and Processing* **20**, 189 (1979).
- [19] J. C. Slater and G. F. Koster, *Phys. Rev.* **94**, 1498 (1954).
- [20] D. J. Chadi, *Phys. Rev. B* **16**, 790 (1977).
- [21] F. Herman, C. D. Kuglin, K. F. Cuff, and R. L. Kortum, *Phys. Rev. Lett.* **11**, 541 (1963).
- [22] F. Herman and S. Skillman, *Atomic structure calculations* (Prentice-Hall, Inc., Englewood Cliffs, New Jersey, 1963).
- [23] R. Leitsmann and F. Bechstedt, *ACS Nano* **3**, 3505 (2009).
- [24] I. Moreels, B. Fritzing, J. C. Martins, and Z. Hens, *Journal of the American Chemical Society* **130**, 15081 (2008).
- [25] V. Petkov, I. Moreels, Z. Hens, and Y. Ren, *Phys. Rev. B* **81**, 241304 (2010).
- [26] G. Bir and G. Pikus, *Symmetry and Strain-Induced Effects in Semiconductors* (Wiley, New York, 1974).
- [27] M. O. Nestoklon, L. E. Golub, and E. L. Ivchenko, *Phys. Rev. B* **73**, 235334 (2006).
- [28] M. Friesen, S. Chutia, C. Tahan, and S. N. Coppersmith, *Phys. Rev. B* **75**, 115318 (2007).
- [29] D. Z. Y. Ting and Y.-C. Chang, *Phys. Rev. B* **38**, 3414 (1988).
- [30] J.-M. Jancu, R. Scholz, G. C. La Rocca, E. A. de Andrada e Silva, and P. Voisin, *Phys. Rev. B* **70**, 121306 (2004).
- [31] C. Bulutay, *Phys. Rev. B* **76**, 205321 (2007).